Multivalent Antibody Fragments with High Functional Affinity for a Tumor-Associated Carbohydrate Antigen[1]

Michael Rheinnecker,[2]* Christina Hardt,* Leodevico L. Ilag,* Peter Kufer,[†] Rudolf Gruber,[†] Adolf Hoess,* Andrei Lupas,[‡] Christine Rottenberger,* Andreas Plückthun,[§] and Peter Pack[3]*

We report in this work a human-derived self-assembling polypeptide based on the tetramerization domain of the human transcription factor p53, which can be fused to single-chain Fv Ab (scFv) fragments via a long and flexible hinge sequence of human origin, allowing exploitation of the functional affinity increase of binding to a ligand or cell surface with multimeric binding sites. We have demonstrated the use of this polypeptide by applying it to the construction of a tetrameric scFv against the tumor-associated carbohydrate Ag Lewis Y (Fucα_1→2Galβ_1→4[Fucα_1→3] GlcNAcβ_1→3R). For comparison purposes, the corresponding scFv and dimeric mini-antibody, comprising the scFv fused via a flexible murine hinge to an artificial dimerization domain, were also created. The recombinant mini-antibody proteins were expressed in functional form in *Escherichia coli* and showed the expected m.w. of a dimer and tetramer, respectively. Analysis of Lewis Y-binding behavior by surface plasmon resonance revealed specific but very weak binding of the scFv fragment. In contrast, both dimeric and tetrameric scFv fusion proteins exhibited an enormous gain in functional affinity that was greatest in the case of the tetrameric mini-antibody.   *The Journal of Immunology*, 1996, 157: 2989–2997.

The presentation of identical antigenic determinants to the immune system in multiple copies on the surface of infectious agents has determined the evolution and architecture of natural Igs. Two to twelve binding sites associate via the constant domains to bi- or multivalent Abs, with rotational and segmental flexibility of the binding arms provided by the hinge regions.

The specific interaction and structural relationship between one Ab binding site and its complementary antigenic determinant are described thermodynamically by the intrinsic affinity. This is the affinity displayed by a monovalent fragment, and with a multivalent fragment it can be measured only with soluble Ags or on surfaces with very low Ag density. In many cases, however, the binding strength between Ab and surface-bound Ag is of direct interest, and it can be enhanced considerably by the formation of multiple binding interactions within one Ab-Ag complex. The term functional affinity was introduced by Karush in 1970 to distinguish between the specific monovalent interaction (the intrinsic affinity) and the enhancement of binding strength by multivalency (1–3). Frequently, the somewhat ill-defined term avidity is used to mean functional affinity.

The enhancement factor between intrinsic and functional affinity is dependent on the intrinsic affinity per binding site, the flexibility and number of the associated binding sites, and the number as well as distance between Ags within reach. Once an Ig has docked to the surface via a single site, the binding of additional binding sites is favored because of their high effective concentrations. As a rough estimate, the functional affinity is the product of intrinsic affinities and local concentrations (4). In case of an anti-DNP IgM, the measured enhancement factor between monovalent and multivalent binding appears in the range of 10^6 to 10^7 (3).

The multivalency effect, however, is not restricted to Igs. For example, the trimeric hepatic lectin (5) binds the trimeric ligand with a 100- to 1000-fold higher functional affinity than the monovalent ligand (6). The functional affinity of the dimeric *Helix Pomatia* A hemagglutinin to its ligand on human A erythrocytes is 10^4-fold higher than the intrinsic affinity of monomeric hemagglutinin, and that of the hexameric structure even 10^6-fold higher (7).

Antibodies against carbohydrates frequently belong to the deca- or dodecavalent IgM class, since carbohydrate Ags are T cell-independent Ags that are usually unable to induce class switching and the ensuing somatic mutations. Given the low intrinsic affinity of most Abs for carbohydrates (8), it is not surprising that, when class switching does occur, most of the murine anti-carbohydrate Abs are switched to the IgG3 class (9) that is known to multimerize via the FcR upon binding to the Ag (10). Similarly, carbohydrate binding by lectins such as conglutinin or IgE-binding protein requires multivalency (11, 12).

A large proportion of relevant tumor-associated Ags are either glycolipids or glycoproteins, in which the carbohydrate epitope plays a predominant role in the Ab-Ag recognition process (13, 14). Unfortunately, carbohydrate-protein interactions are usually of low affinity (8, 15). To date, improvement of carbohydrate binding by protein engineering techniques such as rational design (16) or random mutagenesis (17) leads to only modest improvements and remains challenging.

In this work, we report a novel self-associating polypeptide of human origin, which allows the facile conversion of a single Ag binding site with low intrinsic binding affinity into a tetrameric construct with high functional affinity. For an experimental model

*MorphoSys GmbH, Munich, Germany; [†]Institute of Immunology, Munich, Germany; [‡]Max-Planck Institute of Biochemistry, Martinsried, Germany; and [§]Biochemistry Institute, University of Zurich, Zurich, Switzerland

[2] Current address: Grünenthal GmbH, Steinfeldstrasse 2, D-52222 Stolberg, Germany.

[3] Address correspondence and reprint requests to Dr. Peter Pack, MorphoSys GmbH, Frankfurter Ring 193a, D-80807 Munich, Germany.

system, the scFv[4] derived from the IgM MSL5 was chosen. This Ab binds with low intrinsic affinity to the tumor-associated carbohydrate Ag LeY ($Fuc\alpha_1{\rightarrow}2Gal\beta_1{\rightarrow}4[Fuc\alpha_1{\rightarrow}3] GlcNAc\beta_1{\rightarrow}3R$), which is expressed on a variety of human carcinomas (18, 19) and can be detected on only a few normal tissues, such as gut, at low levels. LeY has also been detected on minimal residual metastatic tumor cells by bone marrow immunocytochemistry (20), and represents a potential target for Ab-based cancer therapy. Using fusions with self-associating polypeptides both of human origin and artificial design, multimeric scFv fusion proteins were produced in *Escherichia coli*, and their binding behavior was compared by ELISA and analysis of surface plasmon resonance.

Materials and Methods

Reagents and cell lines

The murine H18A, a mAb of the IgG3 type, was used as positive control in the LeY-binding studies, and was obtained from Seikagaku Corp. (Medac GmbH, Germany). Immunoblot analysis and ELISA assays were performed using the anti-FLAG Ab M1 (Kodak, New Haven, CT) and anti-mouse IgM- or IgG-specific alkaline phosphatase conjugates (Sigma Chemical Co., St. Louis, MO). Nickel-nitrilotriacetic acid resin for the immobilized metal affinity chromatography was purchased from Quiagen (Hilden, Germany). Restriction and DNA modifying enzymes were from New England Biolabs (Beverly, MA). The LeY-BSA conjugate with an average of 25 tetrasaccharide moieties per albumin molecule, LeX-BSA conjugate with an average of 20 trisaccharide ($Gal\beta_1{\rightarrow}4[Fuc\alpha_1{\rightarrow}3]GlcNAc\beta_1{\rightarrow}3R$) moieties per albumin molecule, and LeY methyl ester were purchased from Alberta Research Council (Edmonton, Canada).

Construction of MSL5 scFv and mini-antibody expression plasmids

rDNA techniques were based on those of Sambrook et al. (21). The MSL5 scFv gene was assembled with the arrangement V_L-$(Gly_4Ser)_3$-V_H via PCR, using the V_H and V_L genes from the hybridoma MSL5 as PCR templates (P. Kufer and G. Riethmüller, unpublished results) in combination with murine V_H- and V_L-specific PCR primers (22). The final PCR product was ligated via *Eco*RV and *Eco*RI into the vector pIG6 (22) to create pMSL5. All pIG-derived vectors (22) have a modular architecture that allows the combination of the MSL5 gene cassette with both an N-terminal sequence coding for a short FLAG epitope (23) and a C-terminal sequence coding for an oligo-His tail for IMAC purification (24) or for self-associating polypeptides (association domains) (22, 25). Each scFv gene is preceded by an *ompA* signal sequence and is under the control of a *lac* promoter/operator.

The dHLXhis gene cassette encoding the dHLX association domain (22) with C-terminal His_6Asn tail for IMAC purification was constructed by add-on PCR. The pMSL5-dHLXhis plasmid for expression of the MSL5-scFv fused to the dHLX association domain (dimeric mini-antibody MSL5-dHLXhis) (25) was prepared by insertion of the dHLXhis gene cassette via *Eco*RI and *Hin*dIII into pMSL5.

The p53his gene, comprising sequences encoding the N-terminal human IgG3 upper hinge (26), residues 319–360 of the human p53 tetramerization domain (27–29), a short linker, and a C-terminal His_5 tail, was synthesized by recursive PCR (30) with the following primers: p53-A (5'-GGGGGGG GGGAATTCACCCCGCTGGGTGACACCACCCACACCTCCGGAAAAC CACTGGAT-3'), p53-B (5'-CAGCTCTCGGAAC ATCTCGAAGCGC TCACGCCCACGGATCTGAAGGGTGAAATATTCTCCATCCAGTGG TTTTCCGGAGG-3'), p53-C (5'-CGAGATGTTCCGAGAGCTGAATG AGGCCTTGGAACTCAAGGATGCCCAGGCTGGGAAGGAGCCAGG GGGGAGC-3'), and p53-D (5'-GGGGGGGGGGGAAGCTTAGACGTCA ATGGTGATGATGGTGCGGCGCGCCTCCGCTCCCCCCTGGCTCC TTCC-3'). The plasmid for expression of the scFv MSL5 fused to the p53 tetramerization domain (tetrameric mini-antibody MSL5-p53his) was constructed by ligation of the p53his gene into pMSL5 via *Eco*RI and *Hin*dIII to create pMSL5-p53his. Both genes encoding the scFv and association

domains are interchangeable for all pIG-derived vectors (22) as *Xba*I-*Eco*RI and *Eco*RI-*Hin*dIII cassettes, respectively.

Expression and purification of MSL5 proteins

The MSL5-IgM was purified from 30 ml of mouse ascites by preparative electrophoresis on a polyvinylchloride-copolymer matrix. IgM was eluted from the corresponding fraction, concentrated, and subsequently purified using a Sephacryl S-400 column (Pharmacia, Uppsala, Sweden) to yield 50 mg of MSL5-IgM of >95% purity (31). The scFv, dimeric, and tetrameric mini-antibodies were expressed in shake flask cultures and purified to homogeneity via IMAC, essentially as described previously for scFv proteins (22, 24). *E. coli* JM83 cells were transformed with each MSL5 construct. Cultures of 4 L were grown in LB medium (Life Technologies, Paisley, U.K.) with 1 M sorbitol and 10 mM betaine at 37°C until OD_{600} of 0.4. The *lac* promotor/operator system was induced with 1 mM of isopropyl β-D-thiogalactopyranoside (IPTG), and the cells continued growth at room temperature for 4 h in case of scFv, and 16 h for both mini-antibody constructs. Whole cell extract was prepared by passing the cell paste twice through a French pressure cell press (SLM Aminco, Urbana, IL). Each MSL5 construct was then purified via IMAC on nickel-nitrilotriacetic acid (Quiagen) using a Biologics HPLC system (Bio-Rad, Hercules, CA). Each purified protein was dialyzed and concentrated in HBS buffer (10 mM HEPES, pH 7.5, 150 mM NaCl, 3.4 mM EDTA). The protein concentration was determined using the calculated molar extinction coefficients (32) at OD_{280} (MSL5-scFv, 56,950 $M^{-1} cm^{-1}$; dimeric mini-antibody MSL5-dHLXhis, 113,900 $M^{-1} cm^{-1}$; and tetrameric mini-antibody MSL5-p53his, 232,920 $M^{-1} cm^{-1}$).

Size exclusion chromatography

A Superose 12 column (Pharmacia) was equilibrated in HBS buffer with a flow rate of 0.5 ml/min. The column was calibrated with standard proteins (cytochrome *c*, 12.4 kDa; carbonic anhydrase, 29 kDa; albumin, 66 kDa; alcohol dehydrogenase, 150 kDa; and β-amylase, 200 kDa). The purified MSL5 constructs were analyzed separately at similar concentrations (MSL5-scFv, 7.5 μM; MSL5-dHLXhis, 2.4 μM; and MSL5-p53his, 1.07 μM).

Functional ELISA assays

Microtiter plates (Nunc, Maxisorp, Wiesbaden, Germany) were coated with 10 μg/ml of either LeY-BSA or LeX-BSA in HBS buffer (50 μl of each solution/well) for 16 h at 4°C. The plates were blocked with PTB and 2% skimmed milk powder for 2 h at room temperature, and washed three times with PBST (PBS buffer, 0.05% Tween). Anti-LeY Ab was incubated on the plate for 90 min at room temperature. For the detection of MSL5 IgM and H18A IgG3, respectively, anti-IgM and anti-IgG alkaline phosphatase conjugates were diluted 1/5000 in PTB, aliquoted (50 μl/well), and incubated for 30 min at room temperature. After three additional washes with PBST, 50 μl of the alkaline phosphatase substrate (4-nitrophenylphosphate) was added to each well, and the OD_{405} was determined using a Dynatech Labs (Chantilly, VA) microtiter plate reader. For detection of recombinant MSL5 proteins via the N-terminal FLAG (23), 50 μl of anti-FLAG-reactive mAb M1 (diluted 1/1000 in PTB) was added to each well and incubated for 45 min at room temperature, followed by three additional washing steps with PBST. The anti-IgG alkaline phosphatase conjugate step and the subsequent development of the assay were performed as decribed above.

Surface plasmon resonance studies

All measurements were conducted in HBS buffer (Pharmacia) with a flow rate of 5 μl/min at 25°C using one sensor cell of a biosensor machine (BIAcore; Pharmacia). LeY-BSA was immobilized covalently on the dextran matrix of a CM5 sensor chip using the standard amine immobilization procedure (33). Following activation of the chip surface with 50 mM N-hydroxysuccinimide and 200 mM N-(dimethylaminopropyl)-N'-ethylcarbodiimide, a LeY-BSA stock solution (155 μg/ml) in PBS was diluted with an equal volume of sodium acetate (1 M, pH 3.0) and injected twice to give a high density surface (7000 RU) of immobilized LeY-BSA. For analysis of the MSL5 proteins, 20 μl of each sample was injected at various concentrations (IgM, 0.3–14 nM; scFv, 0.37–3.75 μM; dimeric mini-antibody, 0.12–2.4 μM; and tetrameric mini-antibody, 0.08–1.07 μM). Dissociation was induced by injection of HBS buffer. Inhibition of LeY binding was analyzed either by addition of soluble LeY Ag to each protein sample before injection or by supplementing the running buffer with LeY during the dissociation phase. The final LeY concentration was always 1 mM. The influence of buffer and protein concentration on the BIAcore signal (bulk effect) was determined by co-injection of various concentrations between 0.5 to 2.5 μM of scFv binding sites, with an excess of soluble Ag (1 mM) in the sample buffer to inhibit binding. The resulting signals reflect the

---

[4] Abbreviations used in this paper: scFv, single-chain Fv antibody fragment; LeY, Lewis Y; LeX, Lewis X; IMAC, immobilized metal affinity chromatography; HBS, (4-(2-hydroxyethyl)-piperazine-1-ethane-sulfonic acid)-buffered saline; PTB, phosphate-buffered saline, 0.05% Tween, and 1% bovine serum albumin; PBST, phosphate-buffered saline and 0.05% Tween; RU, resonance units; obs, observed; diss, dissociation; ass, association; $t_{D1/2}$, time point of half-maximal dissociation; max, maximum.

heavy chains

```
             1     10        20        30        40        50        60        70        80        90       100        110
Chothia numbering                     26,30ab-32              53abc-55                                               96,100,100a-k - 101
             ----------            ------                                                              --------------------
MSL5   QVQLQESGPELKKPGETVKISCKASGYTF..TNYGMNWVKQAPGKGLKWMGWIN..TYTGEPTYADDFKGRVALSLETSASTAYLQINNLKNEDTATYFCAN........DYDGAWFAYWGQGTTVTVSS
H18A   EVKLVESGGGLVQPGGSLKLSCATSGFTF..SDYYMYWVRQTPEKRPEWVAYIS..NGGDIPYYLDTVKGRFTISRDNAKNTLYLQMSRLKSEDTAMYYCAR......GKYDGAWFAYWGQGTLVTVSA
BR55-2 EVKLVESGGGLVQPGGSLKLSCATSGFTF..SDYYMYWVRQTPEKRLEWVAYIS..NGGGSSHYVDSVKGRFTISRDNAKNTLYLQMSRLRSEDTAMYHCAR......GMDYGAWFAYWGQGTLVTVSA
BR 96  EVNLVESGGGLVQPGGSLKVSCVTSGFTF..SDYYMYWVRQTPEKRLEWVAYIS..QGGDITDYPDTVKGRFTISRDNAKNTLYLQMSRLKSEDTAMYYCAR......GLDDGAWFAYWGQGTLVTVSV
B3     DVKLVESGGGLVQPGGSLKLSCATSGFTF..SDYYMYWVRQTPEKRLEWVAYIS..NDDSSAAYSDTVKGRFTISRDNARNTLYLQMSRLKSEDTAIYSCAR......GLAWGAWFAYWGQGTLVTVSV
                               VHCDR1                        VHCDR2                                                    VHCDR3
```

kappa chains

```
             1     10        20        30        40        50        60        70        80        90       100        110
Chothia numbering                     26,27abcdef-32          50-52                                                  91,95abcdef-96
             ---------------        ---                                                            ---------
MSL5   DIQLTQSPLTLSVTIGQPASISCKSSQSLLDS.DGKTYLNWLLQRPGQSPKRLIYLVSKLDSGVPDRFTGSGSG.......TDFTLKISRVEADDLGVYYCWQGTH..FPQTFGGGTKLEIKRA
H18A   DVLMTQTPLSLPVSLGDQASISCCGSSQSIIHT.NGNTYLEWYLQKPGQSPKLLIYKVSNRFSGVPDRFSGSGSG.......TDFTLKISRVEAEDLGVYYCFQGSH..VPFTFGSGTKLEIKRA
BR55-2 DVLMTQTPLSLPVSLGDQASISCRSSQSIVHS.NGNTYLEWYLQKPGQSPKLLISKVSNRFSGVPDRFSGSGSG.......TDFTLKISRVEAEDLGVYYCFQGSH..VPFTFGSGTKLEIKRA
BR96   DVLMTQIPVSLPVSLGDQASISCRSSQIIVHN.NGNTYLEWYLQKPGQSPQLLIYKVSNRFSGVPDRFSGSGSG.......TDFTLKISRVEAEDLEVYYCFQGSH..VPFTFGSGTKLEIKRA
B3     DVLMTQSPLSLPVSLGDQASISCRSSQIIVHS.NGNTYLEWYLQKPGQSPKLLIYKVSNRFSGVPDRFSGSGSG.......TDFTLKISRVEAEDLGVYYCFQGSH..VPFTFGSGTKLEIKRA
                               VLCDR1                        VLCDR2                                                   VLCDR3
```

FIGURE 1. Peptide sequence of the variable domains of MSL5 in comparison with anti-LeY Abs BR55-2 (34), BR96 (35), B3 (36), and H18A (37).

Table I. *Design and peptide sequence of the MSL5 scFv dimeric and tetrameric mini-antibody constructs*

Construct	scFv Fragment	Tag/Hinge	Multimerization Domain	Linker Tag
MSL5-scFv	V_L-$(G_3S)_4$-V_H	myc-H₅		
MSL5-dHLXhis	V_L-$(G_3S)_4$-V_H	PKPSTPPGSS murine IgG3 upper hinge	GELEELLKHLKELLKG – PRK – GELEELLKHLKELLKG helix-1 turn helix-2	H₆N
MSL5-p53his	V_L-$(G_3S)_4$-V_H	TPLGDTTHTSG human IgG3 upper hinge	KPLDGEYFTLQIRGRERFEMFRELNEALELKDAQAGKEP oligomerization domain of human p53 (residues 319-360)	GGSGGAP-H₅

overall bulk influence of soluble LeY, sample buffer, and protein as a function of the injected protein concentration. The bulk effect of soluble LeY alone was determined by injecting it at 1 mM in H_2O. This value was substracted from the measured LeY + buffer + protein values to obtain the contribution of buffer and given protein concentration. After each measurement, the chip surface was regenerated with 10 μl of 2 M guanidinium HCl diluted with an equal volume of HBS buffer.

Results

MSL5 sequence

Assembly PCR of hybridoma cDNA (22) was used to amplify the V_H and V_L of the anti-LeY MSL5-IgM (P. Kufer and G. Riethmüller, unpublished results). For comparison with already characterized anti-LeY Abs, the amino acid sequence of V_H and V_L was aligned manually (Fig. 1) with the sequences of the four anti-LeY Abs BR55-2 (34), BR96 (35), B3 (36), and H18A (37), the latter additionally recognizing the LeY-related stage-specific embryonic Ag (SSEA-1). The V_H of MSL5 shares 54% identity with H18A, 51% identity with BR55-2, and 52% for both BR96 and B3. However, there is a 90% identity among the V_H sequences of H18A, BR55-2, BR96, and B3. The differences between MSL5 and the other LeY-binding Abs lie throughout the entire V_H sequence, but especially in positions 53–59 of CDR2, according to the Chothia numbering (38). The most notable differences are the shorter CDR3 of MSL5 (one amino acid less) and the presence of Asn instead of a conserved Arg at position 96. The comparison of the V_L of MSL5, which is a κ-chain, revealed a higher degree of identity with the other anti-LeY Abs compared with the V_H. MSL5 has a 73% identity with H18A and B3, 71% identity with BR55-2, and 70% identity with BR96, but there is a greater than 95% identity among the other LeY binders. The noticeable differences between the light chain of MSL5 and the other anti-LeY Abs are located in positions 30–33 of CDR1 and 94, 96, and 100 of CDR3.

Molecular design of mini-antibodies

We have expanded the range of self-assembling polypeptide domains (25, 39, 40) by designing a novel association domain incorporating the tetramerization domain of human transcription factor p53. Human p53 consists of four domains (N-terminal transactivation domain, DNA-binding domain, tetramerization domain, C-terminal basic domain). Residues 319–360 of p53 comprise the third domain, which is capable of self associating to a tetramer (27–29).

Oligomerization alone, however, does not automatically result in a dramatic increase in functional affinity of the self-assembled complex, since the oligomer must be geometrically able to bind to several Ags on a solid surface or cell simultaneously. The spatial separation of the p53-derived tetramerization domain from the binding sites by the use of a long and flexible human IgG3 upper hinge provides for independent folding of the fused domains and, even more importantly, for a long reach to bind to distant Ags simultaneously (25, 39, 40).

The product of the assembly PCR of MSL5 encodes an scFv fragment in a V_L-$(Gly_4Ser)_3$-V_H arrangement with an N-terminal *Eco*RV and a C-terminal *Eco*RI restriction site. Recursive PCR was used to synthesize an *Eco*RI-*Hind*III gene cassette encoding the N-terminal human IgG3 upper hinge (26), residues 319–360 of human p53 (27–29) as the tetramerization domain, and a short GGSGGAP linker incorporating an AscI restriction site, followed by a C-terminal His₅ tail (Table I). A schematic representation of the tetrameric mini-antibody expression plasmid pMSL5-p53his and the expression cassette of the MSL-p53his is shown in Figure 2, *A* and *B*, respectively. For comparison, we also constructed the corresponding dimeric mini-antibody MSL5-dHLXhis and the MSL5-scFv. The design of the dHLX gene cassette (25), which codes for a small dimerization domain (6 kDa) based on an artificial helix-turn-helix motif (41), was extended by a C-terminal His

FIGURE 2. *E. coli* expression system. *A*, Schematic overview of the pMSL5-p53his vector constructed for functional expression of the MSL5 tetrameric mini-antibody in *E. coli*. The high copy number phagemid contains the following elements in a clockwise arrangement (22): *lacI* gene encoding the *lac* repressor, MSL5-p53his cistron under a *lac* promoter/operator (*lac* P/O) followed by an *lpp* terminator (term *lpp*), the intergenic region of the f1 phage allowing for production of ssDNA (f1), and *bla* gene encoding β-lactamase for ampicillin resistance and the ColEI origin of replication (ori). *B*, Drawing to scale of the modular MSL5-p53his cistron under the lac promoter (*lac* P, denoted by an arrow) and *lac* operator (*lac* O, drawn as a box). The *lac* P/O is followed by a shortened *lacZ* gene encoding an MTMITNF peptide ending in a stop codon with an *Xba*I restriction site, the *omp*A signal peptide (S) for secretion of the fusion protein into the bacterial periplasm, a FLAG epitope (DYKDI) with an *Eco*RV restriction site for detection, the MSL5 scFv fragment with a $(G_3S)_4$ linker (L) between V_L and V_H domain, an *Eco*RI and *Hin*dIII site for insertion of the human IgG3 hinge cassette (between *Eco*RI and MroI), and the cassette encoding the human p53 tetramerization domain (between MroI and AscI), followed by the His-tail cassette (H_5, between AscI, two stop codons, and *Hin*dIII) in front of the *lpp* terminator.

A

B
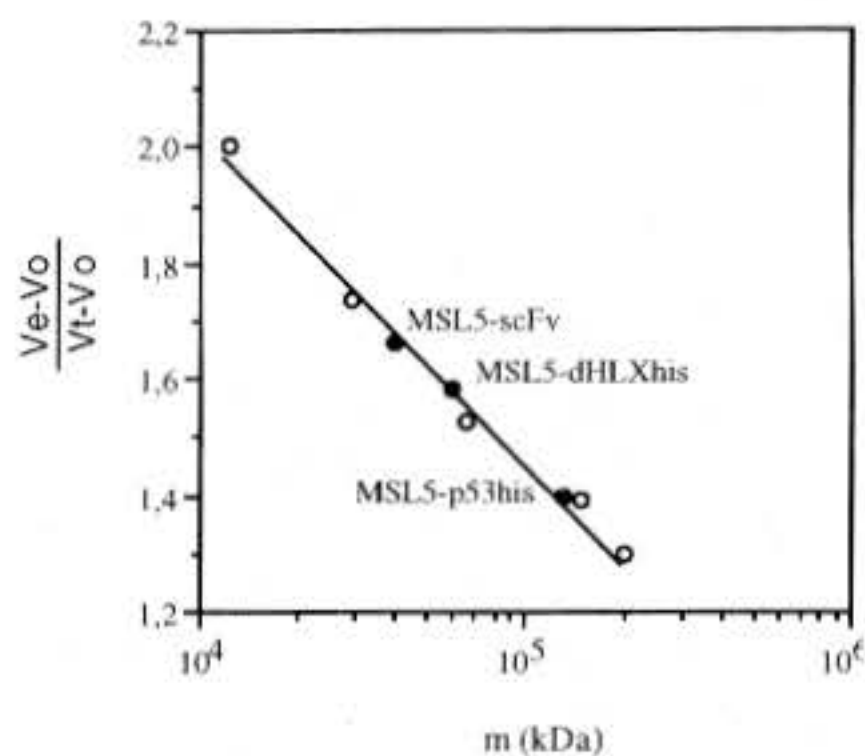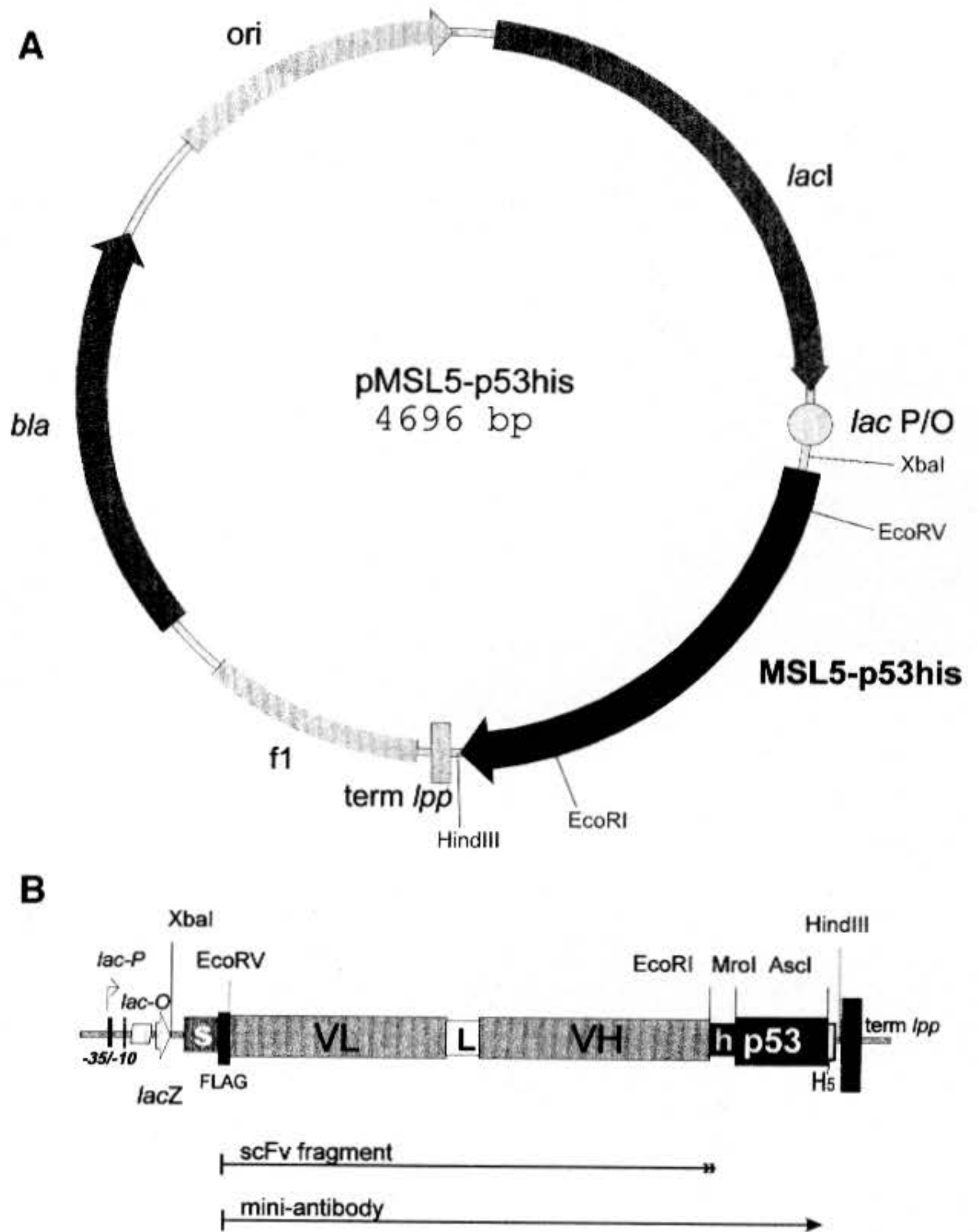
FIGURE 3. Size exclusion chromatography of the MSL5 Ab constructs ($\bullet$) (MSL5-scFv, 7.5 μM; MSL5-dHLXhis, 2.4 μM; MSL5-p53his, 1.07 μM). The column (Superose 12; Pharmacia) was calibrated with standard proteins in HBS ($\bigcirc$) (cytochrome *c*, 12.4 kDa; carbonic anhydrase, 29 kDa; albumin, 66 kDa; alcohol dehydrogenase, 150 kDa; β-amylase, 200 kDa).

tail to allow for purification of the mini-antibody via IMAC (Table I).

Protein expression and purification

The murine MSL5-IgM was purified from mouse ascites (31) by preparative electrophoresis on a polyvinyl chloride-copolymer matrix and a subsequent gel filtration. The recombinant MSL5 mini-

antibody constructs were expressed in *E. coli* in functional yields similar to those of the scFv fragment alone (about 100 μg/L of *E. coli* culture). Each recombinant protein could be purified to homogeneity using standard IMAC (24). The oligomerization state of the constructs was analyzed by gel filtration (Fig. 3). The apparent molecular mass of 40 kDa for the scFv is somewhat higher than the theoretical value (31.4 kDa). This may indicate an equilibrium, fast on the time scale of column chromatography, between an scFv monomer and dimer (42, 43). The apparent molecular masses of the MSL5-dHLXhis (60 kDa) and MSL5-p53his (130 kDa), however, correspond to the expected values of 66.7 kDa (dimer) and 125.5 kDa (tetramer), respectively. The mini-antibodies showed symmetrical peaks, indicating the formation of stable dimers and tetramers.

Functional ELISA with synthetic Lewis Ags

The functionality and specificity of the MSL5 monoclonal, scFv, dimeric, and tetrameric mini-antibody fusions were analyzed on ELISA plates coated with synthetic LeY-BSA and LeX-BSA conjugates. The binding of the MSL5 IgM to synthetic LeY-BSA was similar to that of the murine anti-LeY monoclonal H18A (Fig. 4*A*). Both Abs, however, showed differences in their cross-reactivity with synthetic LeX. Even at high concentrations, the MSL5 monoclonal IgM showed no reactivity with LeX, while cross-reactivity of H18A was apparent at concentrations higher than 10 μg/ml. Both Abs exhibited no binding to milk powder, which was used as
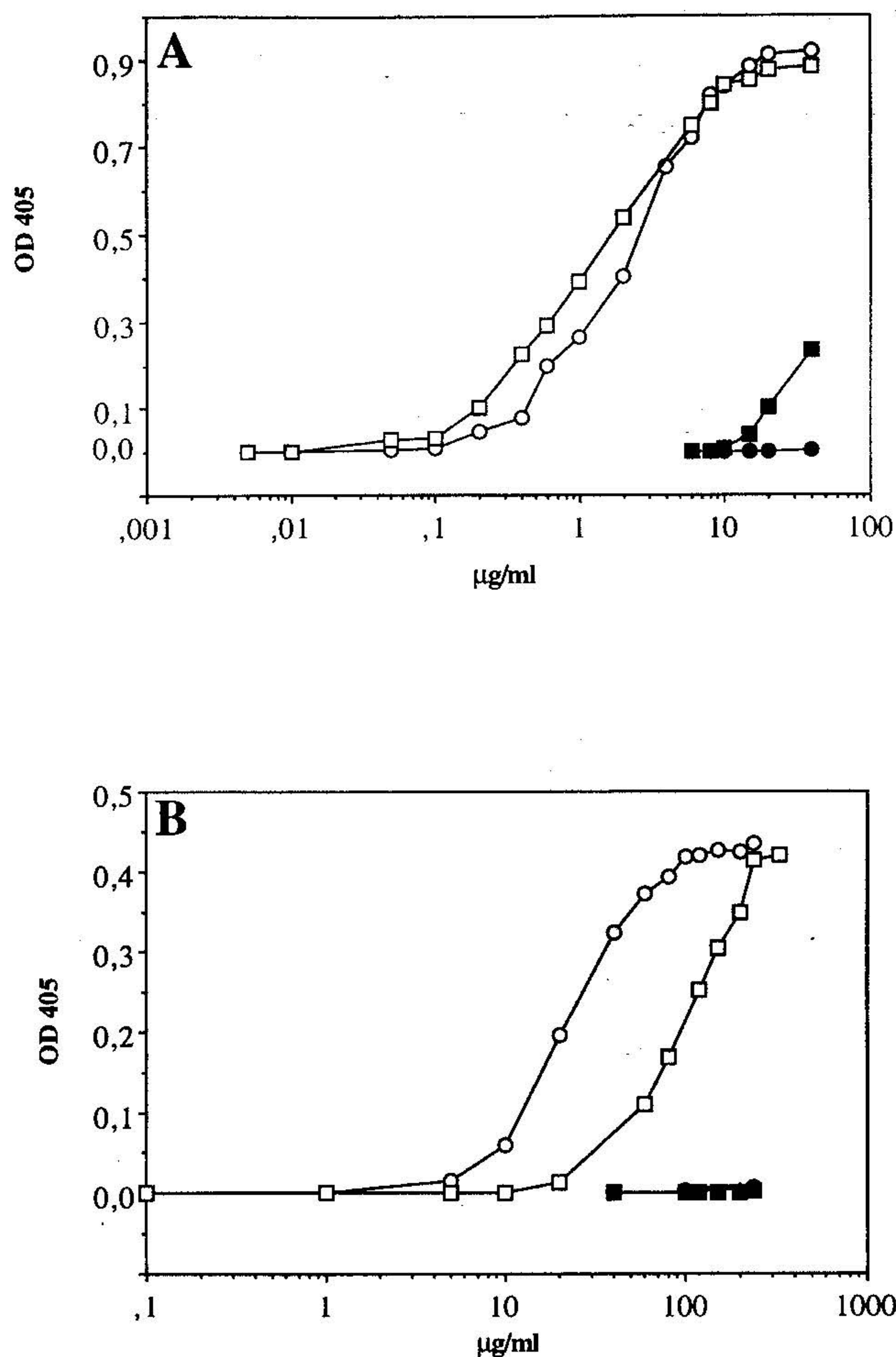
FIGURE 4. *A*, Functional ELISA of mAbs MSL5 IgM (circles) and H18A IgG3 (squares) with LeY-BSA (white symbols) and LeX-BSA Ag (black symbols). The addition of 1 mM of LeY Ag to either H18A and MSL5 (10–40 µg/ml each) resulted in more than 95% reduction of the binding signal to LeY-BSA in each case. Binding of the Abs to milk powder, which was used as the blocking agent, was not detectable (inhibition and milk-powder data not shown). *B*, Functional ELISA of the tetrameric anti-LeY mini-antibody MSL5-p53his (circles) and dimeric anti-LeY mini-antibody MSL5-dHLXhis (squares) with LeY-BSA (white symbols) and LeX-BSA Ag (black symbols). The addition of 1 mM of LeY Ag to both mini-antibody constructs (100–330 µg/ml each) resulted in more than 95% reduction of the binding signal to LeY-BSA in each case. Binding of the Abs to milk powder, which was used as the blocking agent, was not detectable (inhibition and milk-powder data not shown). Bound Abs were detected with either IgM, IgG, or FLAG-specific alkaline phosphatase conjugates.

the blocking reagent. The scFv gave no detectable signal in the LeY-binding assay, despite its potential monomer-dimer equilibrium. In contrast, binding of both mini-antibody proteins was detectable. The stronger ELISA signal of the tetrameric mini-antibody (Fig. 4*B*) in comparison with the dimeric mini-antibody would suggest an additional gain in functional affinity for the tetramer over the dimer. As expected, the specificity of both mini-antibodies is similar to that of the parent monoclonal MSL5 in that no cross-reactivity with LeX-BSA was detectable even at high concentrations of 300 µg/ml. The binding of the MSL5 and H18A monoclonals (10–40 µg/ml) and both mini-antibodies (100–300 µg/ml) to the synthetic BSA-LeY tetrasaccharide could be to more than 95% inhibited in each case by addition of 1 mM of soluble LeY methyl ester (data not shown), indicating specificity.
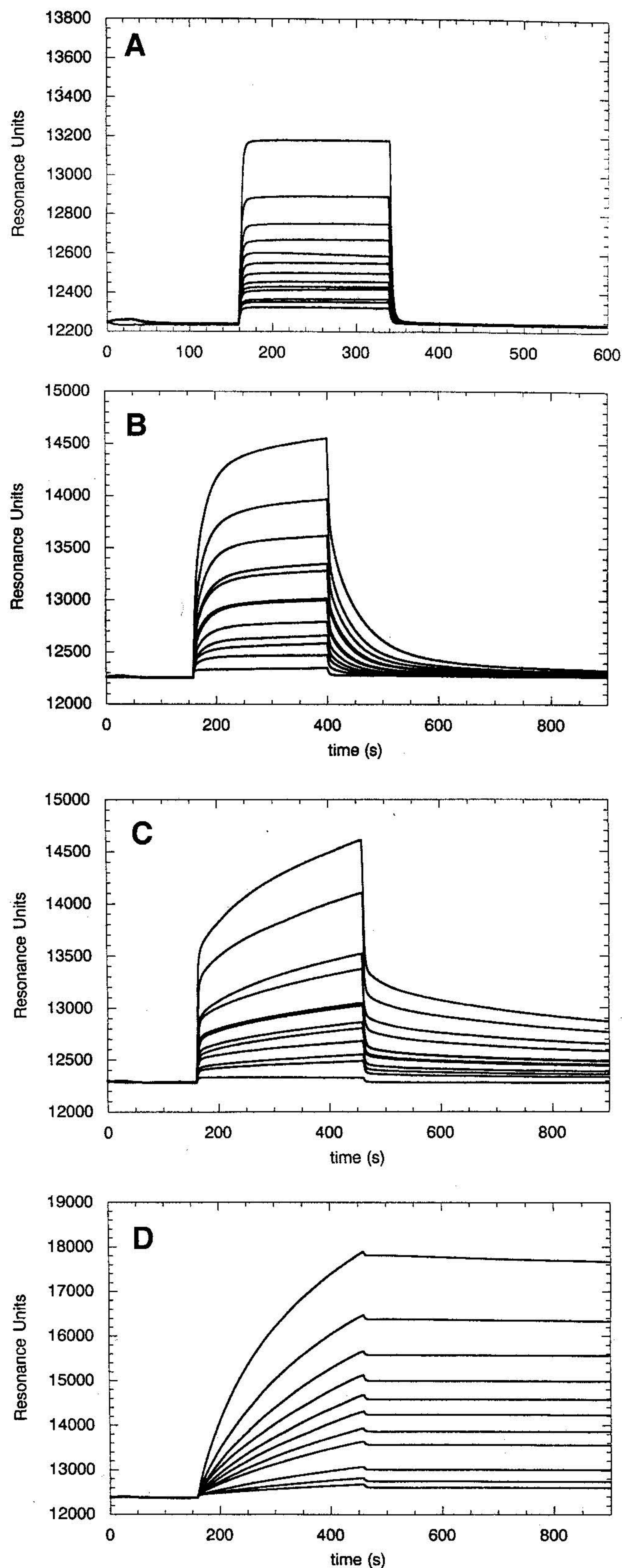
FIGURE 5. Analysis of LeY-BSA-binding behavior of the MSL5-scFv (*A*), dimeric mini-antibody MSL5-dHLXhis (*B*), tetrameric mini-antibody MSL5-p53his (*C*), and MSL5-IgM (*D*) with surface plasmon resonance on a BIAcore biosensor instrument. Shown are overlay plots of each construct at various concentrations (MSL5-scFv, 0.37–3.75 µM; dimeric mini-antibody MSL5-dHLXhis, 0.12–2.4 µM; tetrameric mini-antibody MSL5-p53his, 0.08–1.07 µM; and IgM, 0.3–14 nM).
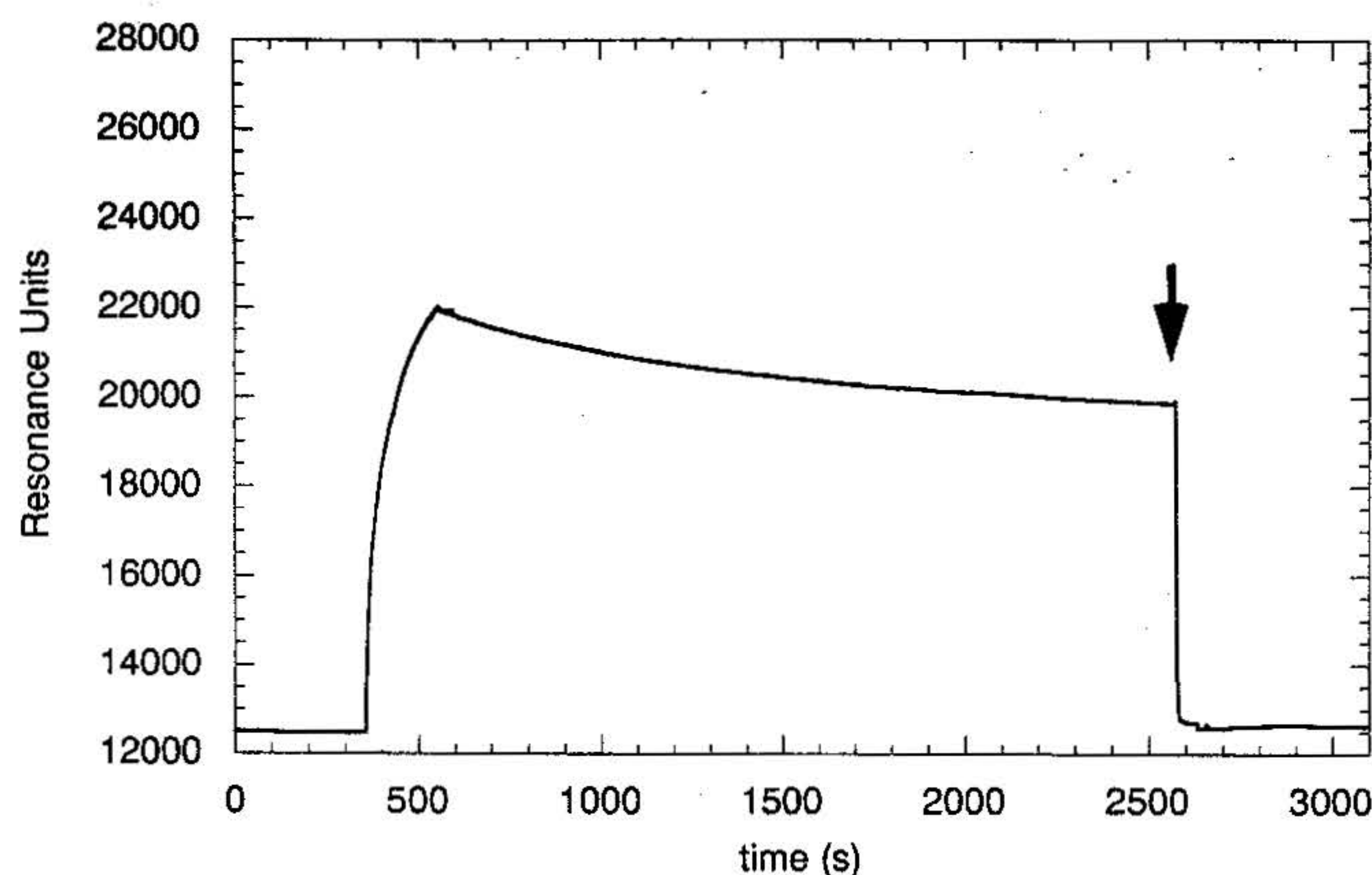
FIGURE 6. Elution of MSL5-IgM (14 nM) from LeY-BSA using soluble LeY Ag. The injection of 1 mM of LeY Ag is indicated by the arrow.

FIGURE 7. Overlay plot of individual dissociation curves of the MSL5-scFv fragment (3.5 μM) (A), dimeric mini-antibody MSL5-dHLX-his (2.4 μM) (B), tetrameric mini-antibody MSL5-p53his (1.07 μM) (C), and the MSL5-IgM (14 nM) (D).

Surface plasmon resonance

The binding of each MSL5 Ig to LeY-BSA was analyzed in real time by surface plasmon resonance (BIAcore) (44). We used experimental conditions of high BSA-LeY Ag density to allow multivalent binding. Even a qualitative analysis of the sensorgrams indicated striking differences in the LeY-binding behavior of the scFv (Fig. 5A) compared with that of the dimeric mini-antibody (Fig. 5B), tetrameric mini-antibody (Fig. 5C), and IgM (Fig. 5D). The scFv fragment exhibited very fast association and dissociation phases, and rapidly reached a steady state of binding, as indicated by the plateau-shaped sensorgrams. This is typical for systems with fast on- and off-rates (BIAcore manual, pp. 8–23 to 8–27). Specific binding of the scFv was apparent, since the signal is larger than the combined bulk refractive indices of buffer and protein in the presence of competing LeY. In contrast, comparison of the sensorgrams from the MSL5 mini-antibody and IgM revealed that both the response rates in the association and dissociation rates decrease as the valency increases.

The decreased on-rate is determined by several factors. First, since the observed rate in the association phase k_{obs} is the sum[5] of the on- and off-rate, $k_{obs} = k_{diss} + [Ab] \cdot k_{ass}$, the observed rate will appear to become slower even if the true k_{ass} is identical, simply because of the decrease in k_{diss} with valency. Second, since the formation of stable bivalent complexes is sterically more demanding, fewer collisions will give rise to them compared with transient monovalent complexes, leading to a decreased k_{ass}. Third, a differential, unspecific interaction of molecules of different size with the dextran matrix of the sensor surface during association cannot be completely excluded.

The intrinsic dissociation rate of the multivalent Igs, which is the microscopic rate constant with which one binding site leaves the Ag, remains very fast, as seen by the instant inhibition with excess of soluble monomeric Ag (Fig. 6) (45). Nevertheless, the observed off-rate also decreases with increasing valency. This is
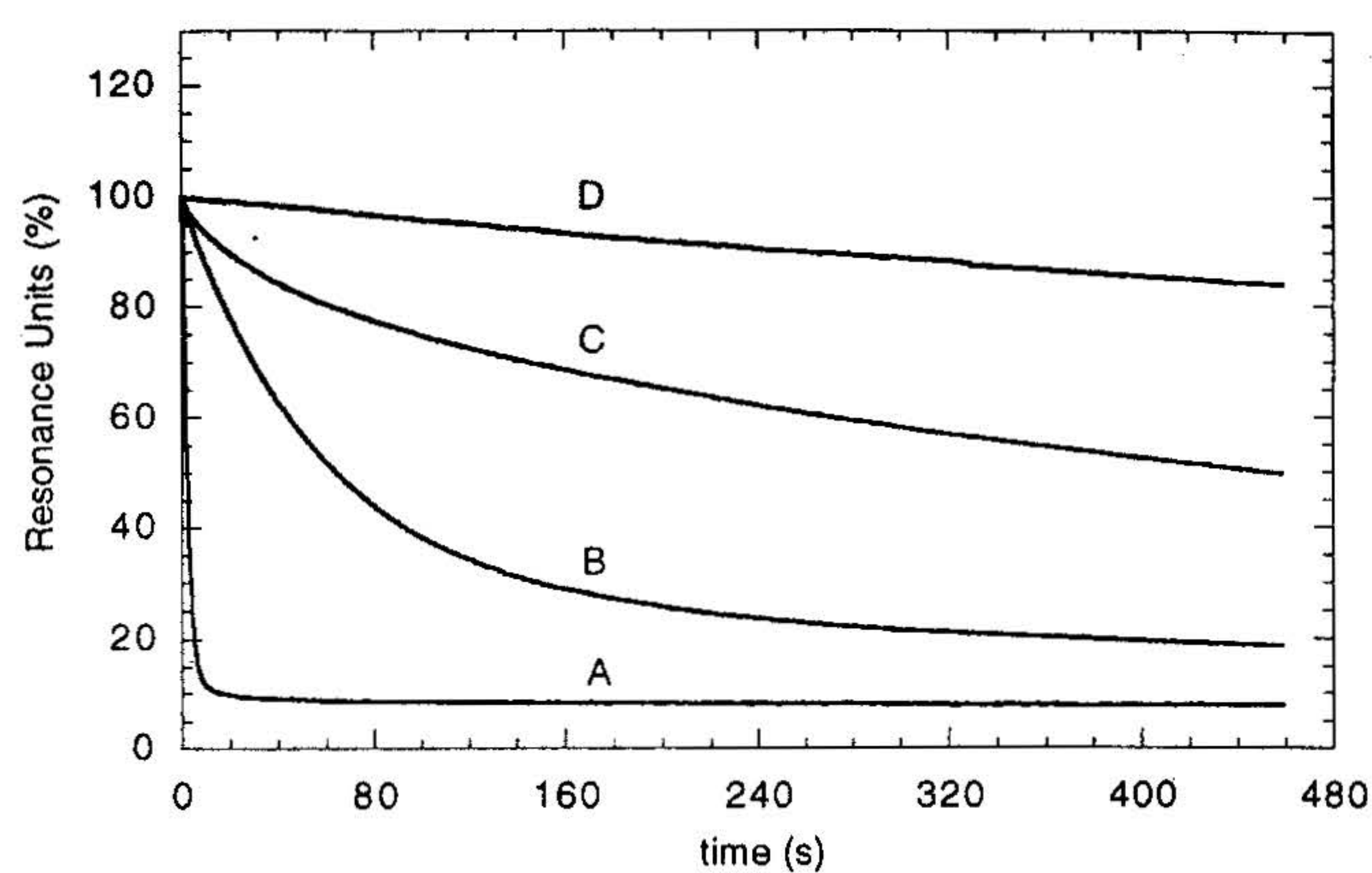
also rooted in several phenomena. Each dissociating arm has a finite probability of rebinding. Thus, with increasing valency the chance increases that at least one of the remaining arms will find a target before the monovalently bound complex dissociates.

Upon complete dissociation, the chance of rebinding to the surface as a dimeric complex also increases with the number of arms. Furthermore, a slow off-rate would of course be expected from true tridentate, or even tetradentate, complexes.

The slowdown in the apparent dissociation with increasing valency is most striking in the case of the decavalent IgM that exhibits the slowest off-rate compared with the dimeric mini-antibody and tetrameric mini-antibody. Furthermore, the overlay plot of selected dissociation curves for each protein (Fig. 7) reveals striking differences in the dissociation behavior, ranging from virtually no dissocation from the LeY-BSA conjugate in the case of the IgM (Fig. 5D) to a nearly instantaneous dissociation exhibited by the scFv fragment (Fig. 5A). In contrast, the very fast dissociation is observed for any fragment, even IgM, if rebinding is prevented by the addition of excess of soluble LeY (Fig. 6). This shows that the differences in the dissociation phase cannot be caused by different diffusion coefficients in the dextran matrix.

The time point of half-maximal dissociation ($t_{D1/2}$), as well as differences in the response signals at the end of the association phase (corrected for the bulk effects of buffer change and protein concentration), can serve as semiquantitative criteria of the multivalency effects under the chosen conditions. At concentrations of about 1 μM binding sites, the specific response (absolute response corrected for the bulk influence of buffer and protein) of the scFv is only 112 RU, whereas the specific signal of the dimeric mini-antibody is eight times higher (889 RU) and that of the tetrameric mini-antibody is about 20 times higher (2120 RU). This is expected, since at 1 μM the scFv concentration is below the estimated intrinsic dissociation constant of about 10 μM, and can therefore not saturate the binding sites, since a steady state is reached. In contrast, because of the slower off-rate, the other proteins do saturate the binding sites, but the response still differs because of differences in mass.

The multivalent binding properties of the tetrameric mini-antibody ($t_{D1/2} = 485$ s) prolong the time span of dissociation by more than two orders of magnitude compared with that of the dimeric mini-antibody ($t_{D1/2} = 70$ s) and the scFv ($t_{D1/2} < 3$ s; Fig. 7). Binding of each multimeric MSL5 Ig to LeY-BSA could be completely and instantaneously inhibited in the presence of soluble $\overset{*}{A}g$, as shown for the immediate dissociation of MSL5-IgM in Figure 6.

---

[5] It is occasionally surmised that in the equation $k_{obs} = k_{ass} \cdot [Ab] + k_{diss}$, there should be a minus instead of a plus sign. It becomes obvious, however, that the sum is indeed correct when the equation is derived (44). The increase of AbAg complex on the surface as a function of time is given by d[AbAg]/dt = {$k_{ass} \cdot$ [Ab] · ([AbAg]$_{max}$ − [AbAg])} − {$k_{diss} \cdot$ [AbAg]}, where [AbAg] is the concentration of bound complex at time t, [AbAg]$_{max}$ is the concentration of bound complex at saturation and ([AbAg]$_{max}$ − [AbAg]) is the concentration of sites still remaining free at time t, and [Ab] is the constant concentration of Ab in the injected sample. Rearrangement of terms gives d[AbAg]/dt = {$k_{ass} \cdot$ [Ab] · [AbAg]$_{max}$} − {$k_{ass} \cdot$ [Ab] · [AbAg] + $k_{diss} \cdot$ [AbAg]}, which can be simplified to d[AbAg]/dt = {Const} − {($k_{ass} \cdot$ [Ab] + k_{diss}) · [AbAg]} or d[AbAg]/dt = Const − $k_{obs} \cdot$ [AbAg], and hence $k_{obs} = k_{ass} \cdot$ [Ab] + k_{diss}. This can be understood from the observed approach to equilibrium being more rapid when both rates are fast.

FIGURE 8. The molecular model of the tetrameric mini-antibody MSL5-p53his was built by fusing the modular components of crystallographic or NMR coordinates of homologous or actual structures. The variable Ab domains of MSL5 are similar (70% kappa, 82% heavy) to those of the anti-progesterone Ab DB3 (PDB entry 1DBA) (54). The sequence of MSL5 was substituted to the DB3 sequence with no major structural adjustments, preserving the Fv interface. The linker was modeled with the structure of murine IgG2a upper hinge. For the structure of the p53 tetramerization domain, NMR coordinates were used (PDB entry 1OLG). All modeling was done with the INSIGHT program (Biosym, MSI, San Diego, CA) and the figure was prepared with MOLSCRIPT.
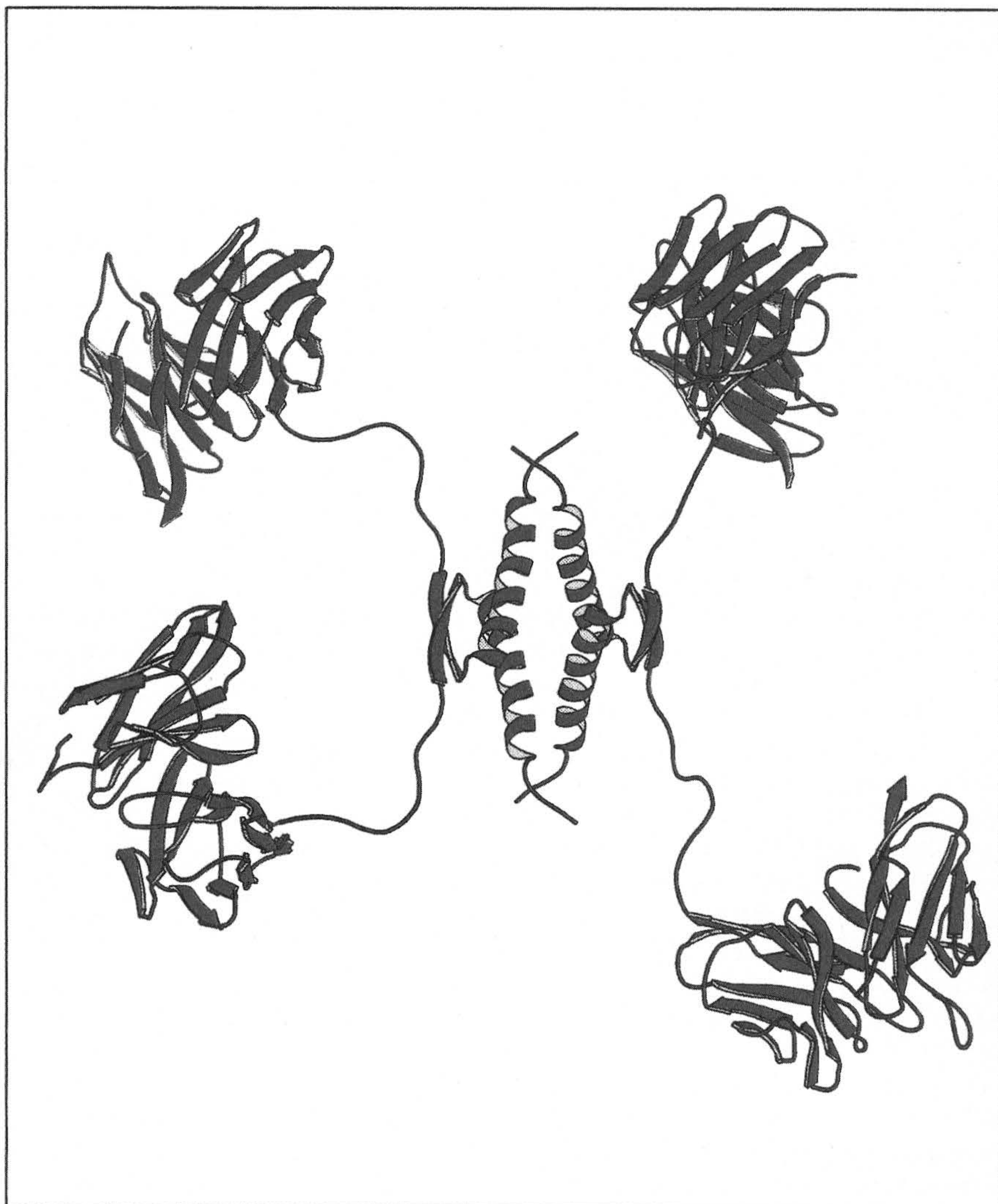
This experiment shows also that the large IgM is not significantly retarded in the matrix, as the intrinsic diffusion is very fast (arrow in Fig. 6). Thus, the intrinsic properties of LeY binding are not changed between any of the constructs, and the observed kinetics are changed exclusively because of binding with higher valency and the rebinding of individual domains and whole molecules observed under these conditions.

Discussion

The multimerization of Ag binding sites has been shown to be an effective means of increasing the functional affinity of bivalent whole Abs (10, 46–48). Multimeric, genetically, or chemically constructed Ab fragments have received considerable attention. A variety of formats has been investigated, such as mini-antibodies (25, 39, 40), diabodies (42, 43, 49), protein A-fusion proteins (50), disulfide-linked fragments (51, 52), or fragments joined with chemically attached spacers (53).

Earlier studies on the design of mini-antibodies, scFv fragments fused via a flexible hinge region to small self-assembling multimerization domains (25, 39, 40), demonstrated the feasibility of this route to self-assembling multivalent Ab fragments with high functional affinities. The initial constructs, however, while proving the principle, might not be ideal for therapeutic applications because of the potential immunogenicity of the previously used association domains, which are based on artificial helix bundles (25) or non-human zipper se-

quences (39, 40). We have therefore designed a novel association domain based on the tetramerization domain of human p53 that is able to combine small size (3.9 kDa), lowest possible immunogenicity, and compatibility with in vivo folding and the formation of stable tetrameric scFv fusion proteins in *E. coli*.

The crystal structure of the p53 tetramerization domain (28) reveals that the tetramer is assembled by two dimers that associate via hydrophobic interactions of α helices and β-strands (Fig. 8). Each dimer, on the other hand, is formed by antiparallel association of two monomers that consist of a β-strand connected to an α helix via a single glycine residue. Clearly, the spider-like model of the tetramerizing mini-antibody based on available structures of p53 (27, 28), human hinges (26), and MSL5 homologous Ab DB3 (54), presented in Figure 8, can only serve as an outline. However, it appears likely that the spatial orientation of the four N termini in the p53 crystal structure, in conjunction with the additional flexibility and reach provided by the human IgG3 upper hinge, would allow, in principle, up to three or perhaps even four fused scFvs to bind simultaneously to distant multimeric Ags. The ELISA and surface plasmon resonance measurements we have reported in this work bear this out, since the tetrameric mini-antibody MSL5-p53his shows significantly stronger binding to immobilized Ag than does the dimeric mini-antibody MSL5-dHLXhis.

A quantitative evaluation of the anti-LeY functional affinities as a function of valency, however, is complicated severely by the

dependence of the multivalent binding behavior on the assay conditions (40), such as Ag density. Furthermore, the rebinding of whole molecules is flow rate dependent in a BIAcore experiment, such that only the relative binding properties under identical conditions are meaningful.

In ELISA measurements, detection of bound mini-antibodies via the N-terminal short FLAG epitope did not allow a direct comparison of signals of dimeric and tetrameric mini-antibodies due to the different number of FLAG tags on both constructs (four FLAG epitopes on the tetrameric mini-antibody vs two epitopes on the dimeric mini-antibody). The weak intrinsic affinity of a single MSL5 binding site (in the form of the scFv) for LeY is apparently not sufficient to survive the repeated washing steps of a functional ELISA. With BIAcore, however, a weak but specific binding signal for the scFv can be detected (Fig. 5A), possibly due to a diabody-like monomer-dimer equilibrium and temporary bivalency. Because of the instantaneous achievement of a steady state indicated by a plateau (as it is typical for such systems (33)), the dissociation constant cannot be obtained from binding kinetics.

Multivalent binding requires conditions of sufficiently high Ag densities that in return will increase the on-rate such that the transport of the Igs to or away from the Ag can become limiting (45). Mass transport limitation may thus in principle lead to an underestimation of the on-rate that becomes apparent by deviations from pseudo-first-order kinetics. Thus, the larger IgM has a somewhat lower diffusion constant, lowering its rate of mass transport compared with the scFv. However, the large differences in the association phase of the different constructs are mainly due to a decreased k_{diss} with higher valency, which is apparent in the association phase because of the simultaneous association and dissociation occurring (see above).

The sensorgrams of the dimeric mini-antibody, tetrameric mini-antibody, and IgM reflect the sum of several multiphasic binding kinetics. Trivalent binding, for example, can be described by several interdependent binding events, each having distinct rate constants. A fast second-order process of the initial collision and monovalent interaction between fragment and Ag is followed either by a fast dissociation (representing the intrinsic affinity) or the first-order formation of a bivalent and thus more stable complex. The first-order transition between monovalent and bivalent binding depends on the accessibility of further Ags, as well as the stability of the monovalent interaction. The bivalent complex either can partially dissociate into the monovalent complex or, favored by the longer resting time of the bivalent complex, form a trivalent complex. Therefore, the reassociation of partially dissociated complexes is highly dependent on the chosen Ag density and flow rate.

In contrast to standard kinetic determinations of thermodynamic affinities in which rebinding distorts calculated values of intrinsic affinities (45, 55), rebinding is of course part of the mechanism by which functional affinity is increased. Thus, the term rebinding does not only refer to the rebinding of completely dissociated Igs, but also to the rebinding of already dissociated binding arms, with one or more arms of the oligomeric construct still binding. The latter phenomenon of functional affinity will be more important, since the local concentration of Ags is much higher for partially dissociated constructs.

A qualitative description of multivalency effects at the chosen conditions can be based on the $t_{D1/2}$. Under identical conditions such as concentration of binding sites, Ag density, and flow rate, the tetrameric mini-antibody reaches a plateau, with about 20 times more binding sites attached to the surface at the end of the association phase than the scFv (Fig. 5). During dissociation, the $t_{D1/2}$ of tetrameric mini-antibody on the chip surface is elongated by a factor of more than 100 (Fig. 7). Since the decameric IgM shows an even longer $t_{D1/2}$ on the chip surface, a further optimization of mini-

antibodies by oligomerization states higher than four could be useful for applications in which only weak intrinsic affinities can be achieved.

All three recombinant MSL5 constructs were expressed in similar functional yields in E. coli. Hence, the expression of either association domain as a C-terminal fusion protein has no detectable influence on secretion or folding of the Ab fragment, and allows assembly of functional multimeric anti-LeY Ab fragments in the periplasm of E. coli. In addition, the C-terminal His tail does not interfere with assembly or stability of either the dimeric or tetrameric mini-antibody, and allows rapid one-step purification via IMAC.

Since the native human p53 transcription factor contains a fourth domain fused C terminally to the tetramerization domain used in this study, it may be possible that a fusion of an effector function to the C terminus will result in a functional tetramer with targeting and effector activities. The crystal structure of the p53 tetramerization domain supports that view in that all four C termini are not only spatially well separated, but project in different directions.

The modular design of the different association domains allows the facile generation of fragments with defined valency and steric properties. For in vivo applications of anti-tumor mini-antibodies, the choice of association domain and oligomerization state should be guided by considerations such as immunogenicity, Ag density on tumor cells, preferred in vivo $t_{1/2}$, and tissue penetration ability. The functional affinity, m.w., and shape of injected Igs determine tissue penetration rates, as well as excretion rate by liver and kidney (56). The dimerization of an anti-phosphocholine scFv into bivalent mini-antibody elongated the plasma $t_{1/2}$ in mice by a factor of two to three compared with a monomeric scFv fragment (57). This correlation of in vivo $t_{1/2}$ and oligomerization state should result in an even further prolonged circulation time in case of the tetrameric, p53-based mini-antibody. This E. coli-expressible mini-antibody format with four binding sites may be an ideal design for applications in which fast excretion and poor functional affinity of a monovalent fragment do not result in a significant, long-lasting enrichment at the target.

Furthermore, the dependence of the functional affinity on the actual Ag density (39) should allow a distinction between different tissues having different Ag densities. LeY is found in high densities on colon and breast cancer cells, but in low densities on a variety of normal cells (18). Since Abs or immunotoxins with higher intrinsic affinity against LeY and related Ags also bind to cell surfaces with low Ag density, significant binding to normal tissues is observed (58). In principle, multimeric mini-antibodies with high functional but comparatively low intrinsic affinities are unable to bind to cells with low densities. Therefore, they should give rise to more selective targeting of cells with overexpressed Ags that favor multivalent binding.

In conclusion, the combination of peptides of human origin, such as the p53 tetramerization domain and a long and flexible hinge, represents a multimerization device that allows the generation of small structures of human origin that self assemble to stable, tetrameric Ab fragments in E. coli. In addition, the use of small association domains for the self assembly of oligomeric structures represents a versatile method for optimizing any proteinaceous receptor-ligand interaction in which binding could be strongly enhanced by multimerization of individual binding sites.

Acknowledgments

References

1. Karush, F. 1970. Affinity and the immune response. *Ann. NY Acad. Sci. 169:56.*

2. Karush, F. 1978. The affinity of antibody: range, variability, and the role of multivalence. In *Comprehensive Immunology*, Vol. 5. G. W. Litman and R. W. Good, eds. Plenum Press, New York, pp. 85–116.

3. Hornick, C. L., and F. Karush. 1972. Antibody affinity. III. The role of multivalence. *Immunochemistry 9:325.*

4. Crothers, D. M., and H. Metzger. 1972. The influence of polyvalency on the binding properties of antibodies. *Immunochemistry 9:341.*

5. Verrey, F., and K. Drickamer. 1993. Determinants of oligomeric structure in the chicken liver glycoprotein receptor. *Biochem. J. 292:149.*

6. Lee, R. T., Y. Ichikawa, T. Kawasaki, K. Drickamer, and Y. C. Lee. 1992. Multivalent ligand binding by serum mannose-binding protein. *Arch. Biochem. Biophys. 299:129.*

7. Hammarström, S. 1973. Binding of *Helix Pomatia A* hemagglutinin to human erythrocytes and their cells: influence of multivalent interaction on affinity. *Scand. J. Immunol. 2:53.*

8. Toone, E. J. 1994. Structure and energetics of protein-carbohydrate complexes. *Curr. Op. Struct. Biol. 4:719.*

9. Elkins, K., and E. S. Metcalf. 1984. Monoclonal antibodies demonstrate multiple epitopes on the O antigens of *Salmonella typhimurium* LPS. *J. Immunol. 133:2255.*

10. Greenspan, N. S., and L. J. Cooper. 1992. Intermolecular cooperativity: a clue to why mice have IgG3? *Immunol. Today 13:164.*

11. Hsu, D. K., R. I. Zuberi, and F. T. Liu. 1992. Biochemical and biophysical characterization of human recombinant IgE binding protein, an S-type animal lectin. *J. Biol. Chem. 267:14167.*

12. Andersen, O., P. Friis, N. E. Holm, K. Vilsgaard, R. G. Leslie, and S. E. Svehag. 1992. Purification, subunit characterization and ultrastructure of three soluble bovine lectins: conglutinin, mannose-binding protein and the pentraxin serum amyloid P-component. *J. Struct. Biol. 109:201.*

13. Feizi, T. 1985. Demonstration by monoclonal antibodies that carbohydrate structures of glycoproteins and glycolipids are onco-developmental antigens. *Nature 314:53.*

14. Hakomori, S. 1984. Tumor-associated carbohydrate antigens. *Annu. Rev. Immunol. 2:103.*

15. Bundle, D. R., and N. M. Young. 1992. Carbohydrate-protein interactions in antibodies and lectins. *Curr. Op. Struct. Biol. 2:666.*

16. Brummell, D. A., V. P. Sharma, N. N. Anand, D. Bilous, G. Dubuc, J. Michniewicz, C. R. MacKenzie, J. Sadowska, B. W. Sigurskjold, B. Sinnott, N. M. Young, D. R. Bundle, and S. A. Narang. 1993. Probing the combining site of an anti-carbohydrate antibody by saturation-mutagenesis: role of the heavy-chain CDR3 residues. *Biochemistry 32:1180.*

17. Deng, S., R. MacKenzie, J. Sadowska, J. Michniewicz, M. N. Young, D. R. Bundle, and S. A. Narang. 1994. Selection of antibody single-chain variable fragments with improved carbohydrate binding by phage display. *J. Biol. Chem. 269:9533.*

18. Sakamoto, J., K. Furukawa, C. Cordon-Cardo, B. Yin, W. J. Rettig, H. F. Oettgen, L. Old, and K. O. Lloyd. 1986. Expression of Lewis[a], Lewis[b], X and Y blood group antigens in human colonic tumors and normal tissue and in human tumor-derived cell lines. *Cancer Res. 46:1553.*

19. Kim, Y. S., M. Yuan, S. H. Itzkowitz, Q. Sun, T. Kaizu, A. Palekar, B. F. Trump, and S. Hakomori. 1986. Expression of LeY and extended LeY blood group-related antigens in human malignant, premalignant and nonmalignant colonic tissues. *Cancer Res. 46:5985.*

20. Schlimok, G., K. Pantel, and G. Riethmüller. 1994. Minimal residual metastatic tumor cells as targets for antibody-based adjuvant therapy of cancer. In *European Association for Cancer Research, EACR XIII Programme and Abstract Book*, pp. 75–82.

21. Sambrook, J., E. F. Fritsch, and T. Maniatis. 1989. *A Laboratory Manual*, 2nd Ed. Cold Spring Harbor Laboratory Press, Cold Spring Harbor, NY.

22. Ge, L., A. Knappik, P. Pack, C. Freund, and A. Plückthun. 1995. Expressing antibodies in *Escherichia coli*. In *Antibody Engineering*, 2nd Ed. C. A. K. Borrebaeck, ed. Oxford University Press, Oxford, pp. 229–266.

23. Knappik, A., and A. Plückthun. 1994. An improved affinity tag based on the FLAG peptide for the detection and purification of recombinant antibody fragments. *Biotechniques 17:754.*

24. Lindner, P., B. Guth, C. Wülfing, C. Krebber, B. Steipe, F. Müller, and A. Plückthun. 1992. Purification of native proteins from the cytoplasm and periplasm of *Escherichia coli* using IMAC and histidine tails: a comparison of proteins and protocols. *Methods 4:41.*

25. Pack, P., M. Kujau, V. Schroeckh, U. Knüpfer, R. Wenderoth, D. Riesenberg, and A. Plückthun. 1993. Improved bivalent mini-antibodies, with identical avidity as whole antibodies, produced by high cell density fermentation of *Escherichia coli*. *Biotechnology 11:1271.*

26. Dangl, J. L., T. G. Wensel, S. L. Morrison, L. Stryer, L. A. Herzenberg, and T. Oi. 1988. Segmental flexibility and complement fixation of genetically engineered chimeric human, rabbit and mouse antibodies. *EMBO J. 7:1989.*

27. Clore, G. M., J. G. Omichinski, K. Sakaguchi, N. Zambrano, H. Sakamoto, E. Appella, and A. M. Gronenborn. 1995. Interhelical angles in the solution structure of the oligomerization domain of p53: correction. *Science 267:1515.*

28. Jeffrey, P. D., S. Gorina, and N. P. Pavletich. 1995. Crystal structure of the tetramerization domain of the p53 tumor suppressor at 1.7 angstroms. *Science 267:1498.*

29. Sakamoto, H., M. S. Lewis, H. Kodama, E. Appella, and K. Sakaguchi. 1994. Specific sequences from the carboxyl terminus of the human p53 gene product form anti-parallel tetramers in solution. *Proc. Natl. Acad. Sci. USA 91:8974.*

30. Prodromou, C., and L. H. Pearl. 1992. Recursive PCR: a novel technique for total gene synthesis. *Protein Eng. 5:827.*

31. Perry, M., and H. Kirby. 1990. Monoclonal antibodies and their fragments. In *Protein Purification Applications*. E. L. V. Harris and S. Angal, eds., IRL Press, Oxford, p. 147.

32. Gill, S. T., and P. H. von Hippel. 1989. Calculation of protein extinction coefficients from amino acid sequence data. *Anal. Biochem. 182:319.*

33. Johnsson, U., L. Fägerstam, B. Ivarsson, B. Johnsson, R. Karlsson, K. Lundh, S. Löfas, B. Persson, H. Roos, I. Rönnberg, S. Sjölander, E. Stenberg, R. Stahlberg, C. Urbaniczy, H. Ostlin, and M. Malmqvist. 1991. Real time biospecific interaction analysis surface plasmon resonance and a sensor chip technology. *Biotechniques 11:620.*

34. Co, M. S., and H. Loibner. 1992. European Patent # 0 528 767 A1, filed August 18, 1992.

35. McAndrew, S. J., L. K. Gilliland, K. M. Ervin, S. M. Webb, H. Wan, H. P. Fell, K. E. Hellström, I. Hellström, and W. L. Cosand. 1996. The carcinoma-reactive monoclonal antibody BR96: cloning, expression and characterization of a single-chain antibody fragment. *Mol. Immunol. In press.*

36. Brinkmann, U., L. H. Pai, D. J. FitzGerald, M. Willingham, and I. Pastan. 1991. B3(Fv)-PE38KDEL, a single-chain immunotoxin that causes complete regression of a human carcinoma in mice. *Proc. Natl. Acad. Sci. USA 88:8616.*

37. Kaneko, T., Y. Iba, K. Zenita, K. Shigeta, K. Nakano, W. Itoh, Y. Kurosawa, R. Kannagi, and K. Yasukawa. 1993. Preparation of mouse-human chimeric antibody to an embryonic carbohydrate antigen, Lewis Y. *J. Biochem. 113:114.*

38. Chothia, C., and A. M. Lesk. 1987. Canonical structures for the hypervariable regions of immunoglobulins. *J. Mol. Biol. 196:901.*

39. Pack, P., and A. Plückthun. 1992. Mini-antibodies: use of amphipathic helices to produce functional, flexibly linked dimeric Fv fragments with high avidity in *Escherichia coli*. *Biochemistry 31:1579.*

40. Pack, P., K. Müller, R. Zahn, and A. Plückthun. 1995. Tetravalent mini-antibodies with high avidity assembling in *Escherichia coli*. *J. Mol. Biol. 246:28.*

41. Hill, C. P., D. H. Anderson, L. Wesson, W. F. deGrado, and D. Eisenberg. 1990. Crystal structure of alpha1: implications for protein design. *Science 294:543.*

42. Whitlow, M., B. A. Bell, S. L. Feng, D. Filpula, K. D. Hardman, S. L. Hubert, M. L. Rollence, J. F. Wood, M. E. Schott, and D. E. Milenic. 1994. An improved linker for single chain Fv with reduced aggregation and enhanced proteolytic stability. *Protein Eng. 7:1017.*

43. Holliger, P., and G. Winter. 1993. Engineering bispecific antibodies. *Curr. Op. Biotech. 4:446.*

44. Karlsson, R., A. Michaelsson, and L. Mattson. 1991. Kinetic analysis of monoclonal antibody-antigen interactions with a new biosensor-based analytical system. *J. Immunol. Methods 145:229.*

45. Glaser, R. W. 1993. Antigen-antibody binding and mass transport by convection and diffusion to a surface: a two-dimensional computer model of binding and dissociation kinetics. *Anal. Biochem. 213:152.*

46. Wolff, E. A., J. Esselstyn, G. Maloney, and H. V. Raff. 1992. Human monoclonal antibody homodimers: effect of valency on in vitro and in vivo antibacterial activity. *J. Immunol. 148:2469.*

47. Shopes, B. 1992. A genetically engineered human IgG mutant with enhanced cytolytic activity. *J. Immunol. 148:2918.*

48. Shuford, W., H. V. Raff, J. W. Finley, J. Esselstyn, and L. J. Harris. 1991. Effect of light chain V region duplication on IgG oligomerization and in vivo efficacy. *Science 252:724.*

49. Perisic, O., P. A. Webb, P. Holliger, G. Winter, and R. Williams. 1994. Crystal structure of a diabody, a dimeric antibody fragment. *Structure 2:1217.*

50. Ito, W., and Y. Kurosawa. 1993. Development of an artificial antibody system with multiple valency using an Fv fragment fused to a fragment of protein A. *J. Biol. Chem. 268:20668.*

51. Carter, P., R. F. Kelley, M. L. Rodrigues, B. Snedecor, M. Covarrubias, M. D. Velligan, W. L. T. Wong, A. M. Rowland, C. E. Kotts, M. E. Carver, M. Yang, J. H. Bourell, H. M. Shepard, and D. Henner. 1992. High level *Escherichia coli* expression and production of a dimeric humanized antibody fragment. *Biotechnology 10:163.*

52. Cumber, A. J., E. S. Ward, G. Winter, G. D. Parnell, and E. J. Wawrzynczak. 1992. Comparative stabilities in vitro and in vivo of a recombinant mouse FvCys fragment and a bisFvCys conjugate. *J. Immunol. 149:120.*

53. Cook, A. G., and P. J. Wood. 1994. Chemical synthesis of bispecific monoclonal antibodies: potential advantages in immunoassay systems. *J. Immunol. Methods 171:227.*

54. Arévalo, J. H., E. A. Stura, M. J. Taussig, and I. A. Wilson. 1993. Three-dimensional structure of an anti-steroid Fab' and progesterone-Fab' complex. *J. Mol. Biol. 231:10.*

55. Nieba, L., A. Krebber, and A. Plückthun. 1996. Competition BIAcore for measuring true affinities: large differences to values determined from binding kinetics. *Anal. Biochem. 234:155.*

56. Thomas, G. D., M. J. Chappell, P. W. Dykes, D. B. Ramsden, K. R. Godfrey, J. R. M. Ellis, and A. R. Bradwell. 1989. Effect of dose, molecular size, affinity, and protein uptake of antibody or ligand: a biomathematical model. *Cancer Res. 49:3290.*

57. Haunschild, J., H. P. Faro, P. Pack, and A. Plückthun. 1995. Pharmacokinetic properties of bivalent mini-antibodies and comparison to other immunoglobulin forms. *Antibody, Immunoconjugates & Radiopharmaceuticals 8:111.*

58. Trail, P. A., D. Willner, S. J. Lasch, A. J. Henderson, S. Hofstead, A. M. Casazza, R. A. Firestone, I. Hellström, and K. E. Hellström. 1993. Cure of xenografted human carcinomas by BR96-doxorubicin immunoconjugates. *Science 261:212.*